Journal Pre-proof

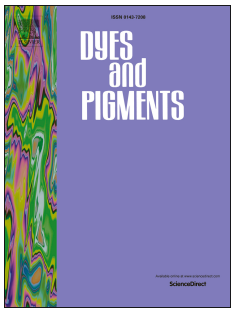

A selective proton transfer optical sensor for copper II based on chelation enhancement quenching effect (CHEQ)

Luís Gustavo Teixeira Alves Duarte, Felipe Lange Coelho, José Carlos Germino, Gabriela Gamino da Costa, Jônatas Faleiro Berbigier, Fabiano Severo Rodembusch, Teresa Dib Zambon Atvars

PII: S0143-7208(20)30304-1

DOI: https://doi.org/10.1016/j.dyepig.2020.108566

Reference: DYPI 108566

To appear in: *Dyes and Pigments*

Received Date: 3 February 2020

Revised Date: 18 May 2020

Accepted Date: 18 May 2020

Please cite this article as: Teixeira Alves Duarte LuíGustavo, Coelho FL, Germino JoséCarlos, Gamino da Costa G, Berbigier JôFaleiro, Rodembusch FS, Zambon Atvars TD, A selective proton transfer optical sensor for copper II based on chelation enhancement quenching effect (CHEQ), *Dyes and Pigments* (2020), doi: https://doi.org/10.1016/j.dyepig.2020.108566.

Author contributions

Luís Gustavo Teixeira Alves Duarte: Conceptualization; Methodology; Formal analysis; Roles/Writing - original draft.

Felipe Lange Coelho: Methodology; Formal analysis; Roles/Writing - original draft.

José Carlos Germino: Formal analysis; Roles/Writing - original draft.

Gabriela Gamino da Costa: Formal analysis; Roles/Writing - original draft.

Jônatas Faleiro Berbigier: Methodology; Formal analysis; Roles/Writing - original draft.

Fabiano Severo Rodembusch: Supervision; Writing - review & editing.

Teresa Dib Zambon Atvars: Funding acquisition; Project administration; Conceptualization; Supervision; Writing - review & editing.

A selective proton transfer optical sensor for copper II based on chelation enhancement quenching effect (CHEQ)

Luís Gustavo Teixeira Alves Duarte,[a†] Felipe Lange Coelho,[b†] José Carlos Germino,[a] Gabriela Gamino da Costa,[b] Jônatas Faleiro Berbigier,[b] Fabiano Severo Rodembusch[b] and Teresa Dib Zambon Atvars[a*]

[a]*Chemistry Institute, University of Campinas, Brazil. E-mail: tatvars@unicamp.br*
[b]*Grupo de Pesquisa em Fotoquímica Orgânica Aplicada, Universidade Federal do Rio Grande do Sul, Porto Alegre, Brazil.*
[†] Authors contributed equally to this work.

Abstract:
A novel selective fluorescent sensor for Cu^{2+} in solution has been developed by means of chelation enhancement quenching effect (CHEQ). The compound *N*,*N*'-bis(salycilidene)-(2-(3',4'-diaminophenyl)benzothiazole (BTS) is reactive to intramolecular proton transfer on the electronic excited state (ESIPT) presenting fluorescence emission in the blue region with very large Stokes shift (8794 cm^{-1}). Spectroscopic titration experiments indicate that not only the fluorescence quenching but also of the ESIPT reaction allowed naked eye detection as a paper strip-based sensor. This chemosensor showed to be selective to Cu^{2+} among 13 other cations. The sensor:Cu^{2+} ratio was determined by both Job and Benesi-Hildebrand plots as 1:2. In addition, the binding between sensor and metal was investigated by ^{1}H NMR, FTIR and HRMS in order to elucidate the formed complex and corroborate the results of BTS:Cu^{2+} ratio. The binding constant was also found as 3.0 x 10^{10} mol^{-2} L^2 at 25°C. The detection and quantification limits were also obtained as 32 ppb and 108 ppb, respectively.

Keywords: benzothiazole; ESIPT; salycilidene, optical sensor; naked eye

1. Introduction

In recent decades, the design and synthesis of different Schiff base-metal complexes was applied mainly in catalysis, biomedicinal sciences and material chemistry [1]. In particular, Salen or Salophen-type, that are tetradentate ligands

showing an almost planar geometry, are able to stabilize different metals, including titanium, zirconium, vanadium, manganese, iron, copper, cobalt, nickel, rhodium, palladium, among others, in various oxidation states [2]. These complexes successfully promoted reactions of carbon-carbon and carbon-heteroatom bond formation, C-H functionalization and a diverse set of chemical transformations [3]. On the other side, the structural features of Salen or Salophen compounds make them suitable for metal cation recognition. Once these compounds present interesting photophysical properties and great affinity for metals, the interaction between sensor and analyte can result in luminescence changes which can be monitored [4]. Among these metals, the present study focus on copper identification, which is still widely used in construction for electrical applications, pipes for industrial flow of fuels, water purification and beverages preparations, or in machine production as an alloy to enhance materials resistance [5,6]. In nature, copper regards significant biochemical processes on every living organism [7,8,9], with a role mainly connected to its redox activity or chemical reactivity where the balance between Cu^{1+} and Cu^{2+} increases its availability due to solubility reasons [10]. Furthermore, it is a cofactor to enzymes that participate on cascade reactions [11] such as respiration [9], photosynthesis [12], neurotransmitter [13] and ATP [14,15] synthesis. Despite being an important micronutrient, the excess of Cu^{2+} or its disbalance between mono and bivalent cations can promote, for instance, neurodegenerative diseases [16,17]. In addition, in food crops such as wheat and rice, depending on the concentration, copper turns a pollutant responsible for growth inhibition and oxidative damage [18]. Thus, to monitor copper presence becomes a relevant issue, where its detection in solution is currently performed by fluorescent probes [19-22]. This metal can be detected as a coordination compound of different ligands, where Schiff bases showed to be useful for this purpose, not requiring complicated synthetic routes and generally using relatively low-cost precursors [33]. These compounds can be envisaged as ligand frameworks with structures easily tuned to bind to cations in solution by mechanisms that might quench (Chelation Enhancement Quenching Effect – CHEQ) or enhance (Chelation Enhanced Fluorescence Effect – CHEF) fluorescence emission [19]. In this context, fluorescence spectroscopy comprises a field in constant development due to its high sensitivity and the possibility of application in many areas including chemistry, biology and medicine [10,19,23-41].

There are several processes that can be responsible for the emission dependence on Cu^{2+} coordination. Specifically, copper can be detected by CHEQ or CHEF mechanisms mainly because of the creation of electronic transitions based on charge transfer from ligand to metal (LMCT – Ligand-Metal Charge Transfer).[19] Moreover, those transitions may be related to either photoinduced electron transfer [23] or to energy transfer processes (resonant or not) [42]. Regardless the process, the fluorescence quenching is described by Yang et al. [43] by CHEQ mechanism in the presence of copper due to its paramagnetic electronic structure [19] and the appearance of a faster and competitive nonradiative deactivation path between LMCT state and the local electronic transition of the ligand.

Herein, we move one step further on the potential technological applications of Schiff bases based on benzothiazole and Salophen moieties that undergoes Excited State Intramolecular Proton Transfer reaction (ESIPT) [44]. In this study, we describe a Salophen sensor selective for Cu^{2+} detection in a high sensibility. Additionally, we also dedicate our efforts to elucidate the complex generated between sensor metal cation by Benesi-Hildebrand and Job plots, as well as spectroscopic analysis.

2. Experimental Procedure

2.1 Materials and Methods

Commercially available reagents were used without further purification. The solvents were purified using standard procedures [45] or used as received. Spectroscopic grade solvents (Merck or Aldrich) were used for the photophysical characterization (UV-Vis absorption and fluorescence emission). All salts were stored under vacuum with dry silica gel for a week before the preparation of the working solutions. Electronic absorption spectra were recorded with the Hewlett-Packard 8452A diode array spectrophotometer. Fluorescence emission spectra were performed by ISS single-photon counting spectrofluorimeter model PC1 in a quartz cuvette with 1 cm of optical path, respectively. Samples were placed in the Hewlett-Packard 89090A Peltier temperature controller set at 25 ^{o}C for 5 min before analysis and metal ions addition. A stock solution of BTS 4.0 µmol L^{-1} in a mixture of acetonitrile and deionised water ($MeCN/H_2O$) 7:3 v/v was employed. Along with solutions of chloride salts from the cations sodium, potassium, lithium, barium, calcium, magnesium, cadmium, tin (II), nickel, aluminium, copper (II), mercury (II) and silver nitrate 5.0 mmol L^{-1} in deionised

water or pure acetonitrile for the last two. Deionised water was obtained from Direct-Q3 UV deionizer from Millipore® with 18.2 mΩ of conductivity.

^{1}H NMR and ^{13}C NMR spectra were recorded in $CDCl_3$ or DMSO-d_6 solutions on a Varian 400 MHz and Bruker 400 MHz spectrometers. Chemical shifts (δ) are given in part per million from the peak of tetramethylsilane (δ=0.00 ppm) as internal standard in ^{1}H NMR or from the solvent peak of $CDCl_3$ (δ=77.23 ppm) in ^{13}C NMR. Data are reported as follows: chemical shift (δ), multiplicity, coupling constant (J) in Hertz and integrated intensity. High resolution mass spectra (HMRS) were recorded on a Micromass Q-Tof spectrometer, using electrospray ionization (ESI). FTIR spectra were recorded on a Varian 640-IR using KBr disc or at ATR mode. Purification by column chromatography was carried out on silica gel 60 (230−400 mesh). Analytical thin-layer chromatography (TLC) was conducted on aluminium plates with 0.2 mm of silica gel 60F-254. Melting points were determined on a Büchi Melting Point M-545.

2.2 Synthesis and spectroscopic characterization

Bis(2-aminophenyl)disulfide (**2**)

A suspension of benzo[d]thiazol-2-amine (**1**) (numbers for compounds identification were shown in Scheme 1) (2.0 g, 11.1 mmol) in 15 mL of aqueous solution of NaOH (10 M) was refluxed for 24 h. After cooling, mixture was filtered and filtrate was acidified with concentrated HCl to pH 2-3 and stirred for 10 min. After, solids were separated out and solution was neutralized with K_2CO_3 and kept crystallizing overnight. Filtration gave 1.03 g (60 % yield) of desired product as yellow crystals. ^{1}H NMR (400 MHz, $CDCl_3$): δ 7.19-7.12 (m, 4H), 6.70 (d, *J*=7.09 Hz, 2H), 6.58 (t, *J*=7.09 Hz, 2H), 4.32 (s, 4H); ^{13}C NMR (100.7 MHz, $CDCl_3$): δ 148.5, 136.9, 131.6, 118.7, 118.3, 115.1.

2-(3',4'-diaminophenyl)benzothiazole (**4**)

In 50 mL of dry toluene was dissolved disulfide **2** (1.0 mmol) and PBu_3 (2.0 mmol) and stirred for 10 minutes. After 3,4-diaminobenzoic acid (1.0 mmol) was added and the mixture was refluxed for 48 h. After cooling, reaction was diluted with 40 mL of ethyl acetate and washed with concentrated $NaHCO_3$ solution (2x45 mL) and water (2x45 mL). The organic phase was separated, dried with Na_2SO_4 and concentrated under vacuum. The residue was purified by column chromatography on silica gel using dichloromethane/ethyl acetate (50:50) as eluent. The product was obtained as white

purple crystals in 82% yield. ^{1}H NMR (400 MHz, DMSO-d_6): δ 8.00 (d, *J*=8.05 Hz, 1H), 7,88 (d, *J*=8.05 Hz, 1H), 7.44 (t, *J*=7.61 Hz, 1H), 7.33 (t, *J*=7.61 Hz, 1H), 7.32 (d, *J*=2.00 Hz, 1H), 7.17 (dd, *J*=8.00 Hz, 2.00 Hz, 1H), 6.60 (d, *J*=8.22 Hz, 1H), 5.24 (s, 2H), 4.81 (s, 2H). ^{13}C NMR (100.7 MHz, DMSO-d_6): δ 169.2, 154.3, 139.7, 135.2, 134.2, 126.6, 124.7, 122.2, 122.1, 122.0, 118.5, 114.1, 113.1.

N,*N*'-bis(salycilidene)-(2-(3',4'-diaminophenyl)benzothiazole (**6**)

In a Schlenk tube, 2-(3',4'-diaminophenyl)benzothiazole (2 mmol) and salicylaldehyde (8 mmol) were dissolved in ethanol and kept at reflux temperature for 24 h. The desired product (**6**) was purified using a Soxhlet extractor with ethanol as the solvent and isolated with 90% yield as an orange powder. The product (**6**) was recrystallized from hot ethanol solution followed by drop-wise addition of hot tetrahydrofuran (THF) until complete solubilization. M.p.: 224–226 °C. ^{1}H NMR (400 MHz, DMSO-d_6): δ 12.76-12.80 (s, 1H), 12.72-12.76 (s, 1H), 9.08-9.10 (s, 1H), 9.01-9.03 (s, 1H), 8.15-8.19 (d, 1H, *J*=8.0 Hz), 8.07-8.13 (t, 3H, *J*=7.5 Hz), 7.75-7.78 (dd, 1H, *J*=7.5 Hz and *J*=1.5 Hz), 7.70-7.73 (dd, 1H, *J*=7.5 Hz and *J*=1.5 Hz), 7.62-7.66 (d, 1H, *J*=8.5 Hz), 7.55-7.60 (t, 1H, *J*=7.5 Hz), 7.47-7.51 (t, 1H, *J*=7.5 Hz), 7.42-7.47 (t, 2H, *J*=8.0 Hz), 6.97-7.02 (m, 4H). ^{13}C NMR (100.7 MHz, DMSO-d_6): δ 207.2, 166.9, 165.3, 164.9, 160.9, 160.9, 154.0, 145.2, 143.7, 135.1, 134.4, 134.2, 133.0, 132.9, 132.5, 127.3, 127.0, 126.2, 123.3, 122.9, 121.2, 120.0, 119.8, 119.7, 118.6, 117.2, 117.2. FTIR (cm^{-1}): 3058, 1609-1592, 755. HRMS (ESI) calcd for $C_{27}H_{20}N_3O_2S$ requires 450.1232 m/z, found 450.1229 m/z $(M+H)^+$.

2.3 Determination of limits of detection (LD) and quantification (LQ)

The determination of BTS:Cu^{2+} ratio and the binding constant for the coordination compound formation were performed in terms of Benesi-Hildebrand and Job plots. The limits of detection (LD) and quantification (LQ) were calculated based on fluorescence titration of BTS to the linear response region of the plot F/F_0 *vs* $[Cu^{2+}]$, according to the Equations (1) and (2):

$$LD = \frac{3S}{b} \quad (1)$$

$$LQ = \frac{10S}{b} \quad (2)$$

where S is the standard deviation of the curve linear coefficient and b is the angular coefficient [46]. To visualize the quenching process and evaluate the possibility of the use as a sensor, paper filter strips of ± 1.0 cm² were immersed initially in BTS MeCN/H_2O (7:3 v/v) solution dried in air and subsequently immersed in the respective salt solutions. Samples were irradiated by a commercial UV-lamp before and after the addition of ions.

3. Results and Discussion

3.1 Synthesis

The synthetic route for obtaining the compound *N*,*N*'-bis(salycilidene)-(2-(3',4'-diaminophenyl)benzothiazole (**6**), so-called BTS, is presented in Scheme 1. The synthesis starts from the hydrolysis of the benzothiazole **1** with aqueous sodium hydroxide to produce the disulfide **2**. Compound **2** was reacted with 3,4-diaminobenzoic acid (**3**) on reflux in presence of tributylphosphine that promotes disulphide cleavage and coupling with the carboxylic acid to afford the compound **4** [47]. The condensation between diamine derivative **4** and salicylaldehyde (**5**) in ethanol under reflux leads to formation of the product **6** in 90% yield, which was first purified using a Soxhlet extraction system using ethanol as solvent, followed by recrystallization with ethanol/tetrahydrofuran.

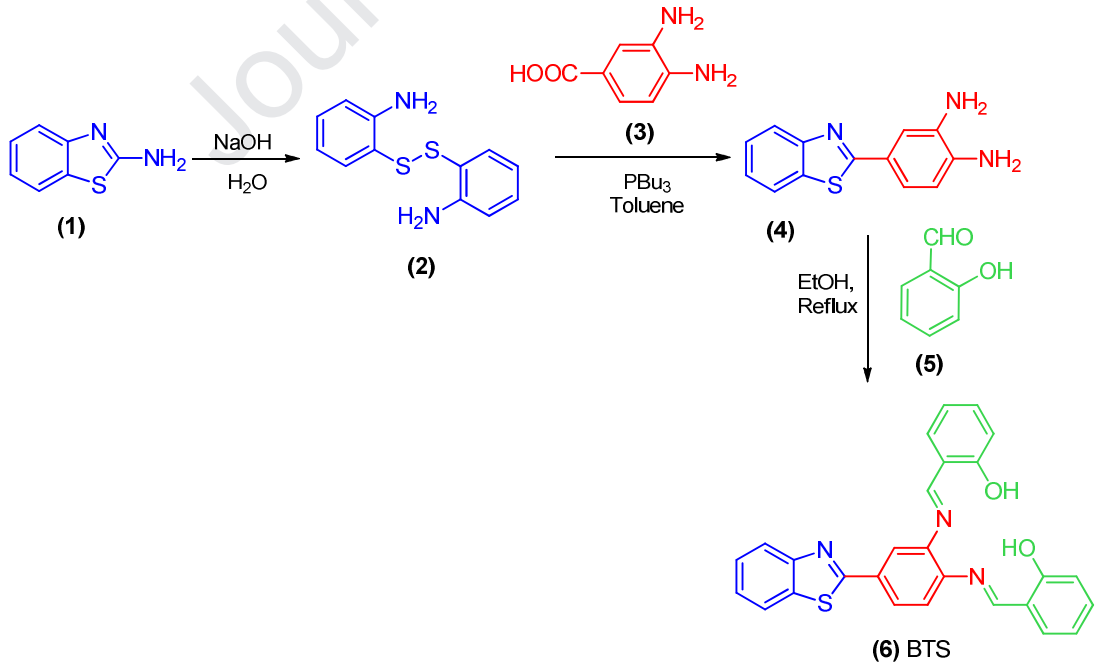

Scheme 1. Synthetic methodology for obtaining BTS (**6**).

3.2 Photophysical characterization

As previously described for dichloromethane (DCM) solution [44], BTS is highly reactive to ESIPT process. In MeCN/H_2O (7:3 v/v) solution (4.0 µmol L^{-1}), the ligand kept its absorption band with maximum centered at 340 nm. It was observed a slight blue shift due to media polarity increase when compared to DCM, once intramolecular hydrogen bond stability between the iminic nitrogens and hydroxyls moieties are committed (Figure 1a). Fluorescence emission profile (λ_{exc} = 340 nm) in MeCN/H_2O (7:3 v/v) solution is similar to the spectrum obtained in DCM solution, presenting a triple emission profile with maxima centered at 390 nm, 485 nm and 520 nm related to the enol form N*, tautomeric T* and anionic A* forms, respectively. N* is the locally excited species, T* form arises from the ESIPT reaction (Figure 1b) and A* is due to deprotonation at electronic ground state [44].

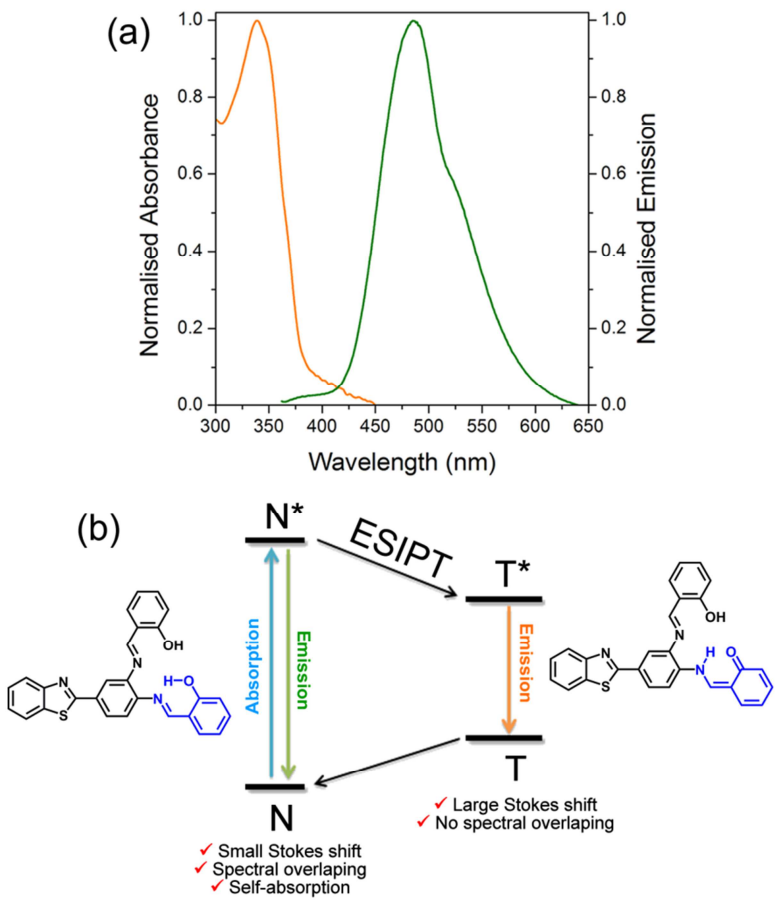

Figure 1. (a) Normalised electronic UV-Vis absorption and fluorescence emission spectra of BTS in MeCN/H_2O (7:3 v/v) solution (4.0 µmol L^{-1}, λ_{exc} = 340 nm) and (b) ESIPT photochemical cycle.

3.3 Metal Ion Recognition

BTS in MeCN/H_2O (7:3 v/v) solution was applied as optical sensor for metal ion detection. To the BTS solution (4.0 µmol L^{-1}) 11 equivalents from the ion solutions (5.0 mmol L^{-1}) were independently added. The fluorescence spectra of these mixtures were acquired with λ_{exc} = 340 nm and their intensities (F) were related to pure BTS emission in the absence of the ions (F_0) as presented in Figure 2. It can be observed that all studied ions presented F/F_0 ratio higher than 0.5. However, in presence of copper, the BTS fluorescence intensity decreases significantly presenting an F/F_0 ratio close to zero, indicating the sensitivity and selectivity of BTS to copper (II).

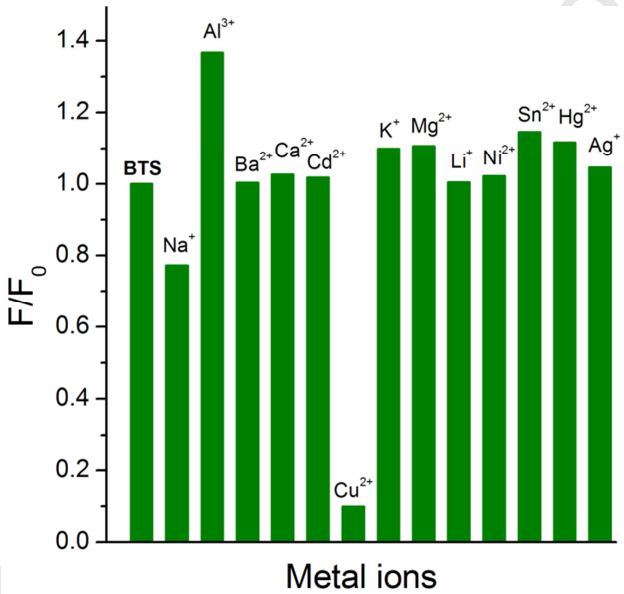

Figure 2. Histogram of BTS normalised fluorescence response upon the addition of various cations in MeCN/H_2O (7:3 v/v) solution where BTS is the normalised emission intensity (F_0) in the absence of ions and F the emission after metal addition.

3.4 Spectroscopic titrations

Based on the photophysical results of BTS in presence of copper II, its ability to bind to BTS was evaluated by spectroscopic titration with metal ion addition. In this sense, spectroscopic titration experiments were employed in terms of Job and Benesi-Hildebrand plots by the acquisition of electronic absorption and emission spectra, respectively. Regarding the absorption spectra along the addition of Cu^{2+} (Figure 3a), it was observed a decrease of BTS absorption intensity at the maxima wavelength (340 nm).

Using the normalised absorption spectra, the Job plot was constructed with the λ_{abs} = 334 nm against the molar fraction of Cu^{2+} (X_{Cu}^{2+}) and offered the proportion between ligand and metal ion as 1:2 (Figure 3b).

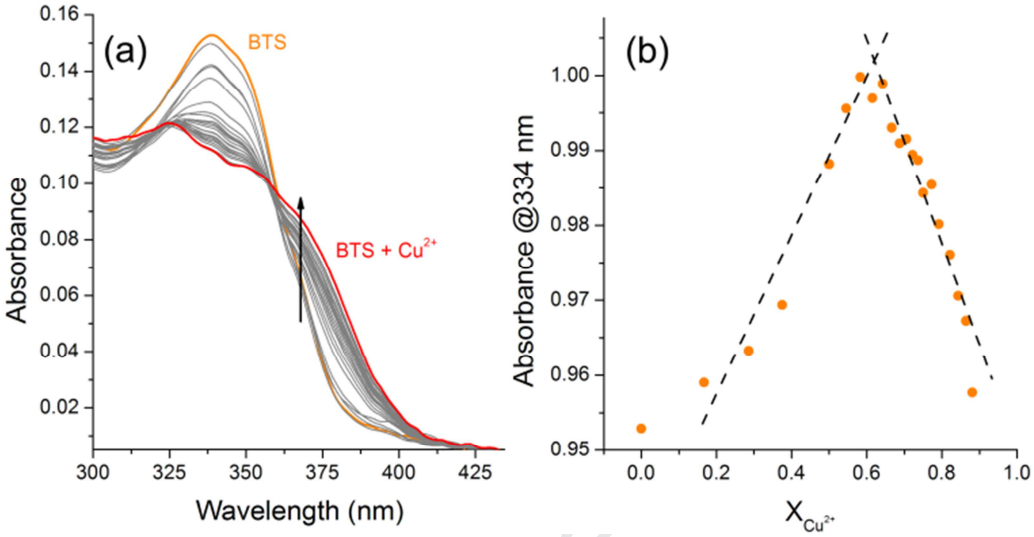

Figure 3. (a) Electronic absorption spectra dependence on the addition of Cu^{2+} and (b) Job plot using the normalised absorbance at 334 nm to X_{Cu2+} = 0.00 to 0.88 Eq. BTS concentration: 4.0 μmol L^{-1}.

The fluorescence emission spectra upon the addition of Cu^{2+} (Figure 4) indicate the occurrence of CHEQ process. The quenching occurs mostly at the emission region of the tautomeric species (T*) of BTS (λ_{em} = 485 nm). It is worth mentioning that A* species is still present after Cu^{2+} addition with λ_{em} = 540 nm and an additional band centered at λ_{em} = 425 nm was observed, which will be addressed later on. Hence, it was assumed that Cu^{2+} is not inducing deprotonation of BTS prior to coordination in MeCN/H_2O (7:3 v/v) solution, but only disfavouring the ESIPT balance. To the construction of Benesi-Hildebrand plot, it was considered the following chemical reaction:

$$BTS + nCu^{2+} \rightarrow Y, \quad (3)$$

where Y is the coordination compound and *n* stands for the stoichiometric proportion between ligand and Cu^{2+}. Hence, the binding constant K_{bind} of Y can be determined by Equation (4).

$$K_{bind} = \frac{[Y]}{[BTS][Cu^{2+}]^n} \quad (4)$$

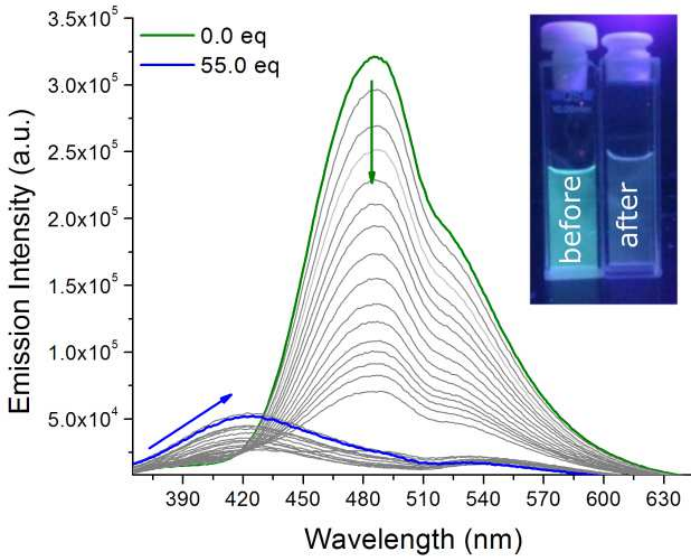

Figure 4. Electronic emission spectra dependence on the addition of Cu^{2+} until 55.0 Eq. of BTS initial concentration (4.0 μmol L^{-1}, λ_{exc} = 340 nm). The inset presents two cuvettes with and without the addition of Cu^{2+} under a UV-lamp light for visual comparison.

Assuming that the concentration of free ions is equal to its total amount in solution and the fluorescence intensities (F) are directly proportional to the concentrations of Y and BTS, K_{bind} can be deduced using Equation (4) as follows:

$$\frac{F - F_0}{F - F_f} = \frac{[Y]}{[BTS]} = K_{bind}[Cu^{2+}]^n \quad (5)$$

where F_0, F and F_f are the fluorescence intensities without Cu^{2+} addition, along Cu^{2+} addition and at final Cu^{2+} addition in the titration experiment using λ_{em} = 485 nm, respectively [36,48]. After taking the module and linearizing Equation (5), the logarithmic form of Benesi-Hildebrand plot was finally constructed (R^2 = 0.98671, Figure 5a) to the region where the plot F/F_0 vs $[Cu^{2+}]$ is a straight line (R^2 = 0.98002). The linear plot resulted in n = 2.0 and K_{bind}= 3.0 x 10^{10} mol^{-2} L^2 at 25°C, in agreement with the absorption experiments. From Figure 5b we determined both the detection and

quantification limits using Equations (1) and (2) as LD = 32 ppb and LQ = 108 ppb, which are comparable to the values found in the literature [36].

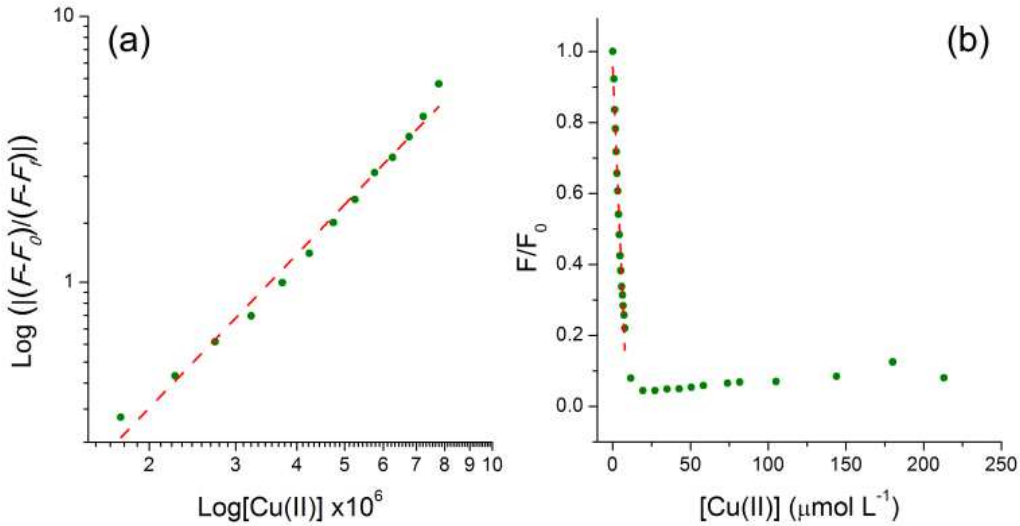

Figure 5. (a) Benesi-Hildebrand plot (R^2 = 0.98671) to the range of concentration of Cu^{2+} from 7.4 x 10^{-7} mol L^{-1} to 8.0 x 10^{-6} mol L^{-1} and (b) F/F_0 vs [Cu^{2+}] (R^2 = 0.98002) to the range of concentration of Cu^{2+} from 0.74 µmol L^{-1} to 220 µmol L^{-1} using the emission intensity at 485 nm. BTS concentration: 4.0 µmol L^{-1}.

In order to understand the unusual proportion between BTS and Cu^{2+}, found as 2:1, respectively, for Salophen-type ligands [49,50], and the extra emission band (λ_{em} = 425 nm) additional experiments were performed in attempt to characterize the generated complex. In this way, spectroscopic and spectrometric analysis were performed in samples containing 0.25 to 2.0 Eq. of Cu^{2+}. Firstly, from the ^{1}H NMR analysis (Figure 6, and Figures S1-S3), it was clearly observed that even at low Cu^{2+} concentration (0.25 Eq.) the imine group of the BTS hydrolyses. The presence of hydrogens of aldehyde C-H bond and hydroxyl group of salicylaldehyde in the ^{1}H NMR spectrum corroborate with the proposed hydrolysis. Furthermore, the intensity of corresponding signals increased as the amount of Cu^{2+} is raised. Also, the presence of a broad singlet located at 5.7-5.4 ppm, as well as the vibrational band located at 4300 cm^{-1} in FTIR spectrum (Figure S4), assigned to secondary amine symmetric stretching, overlapped by O-H stretching, confirm the presence of NH_2 group.

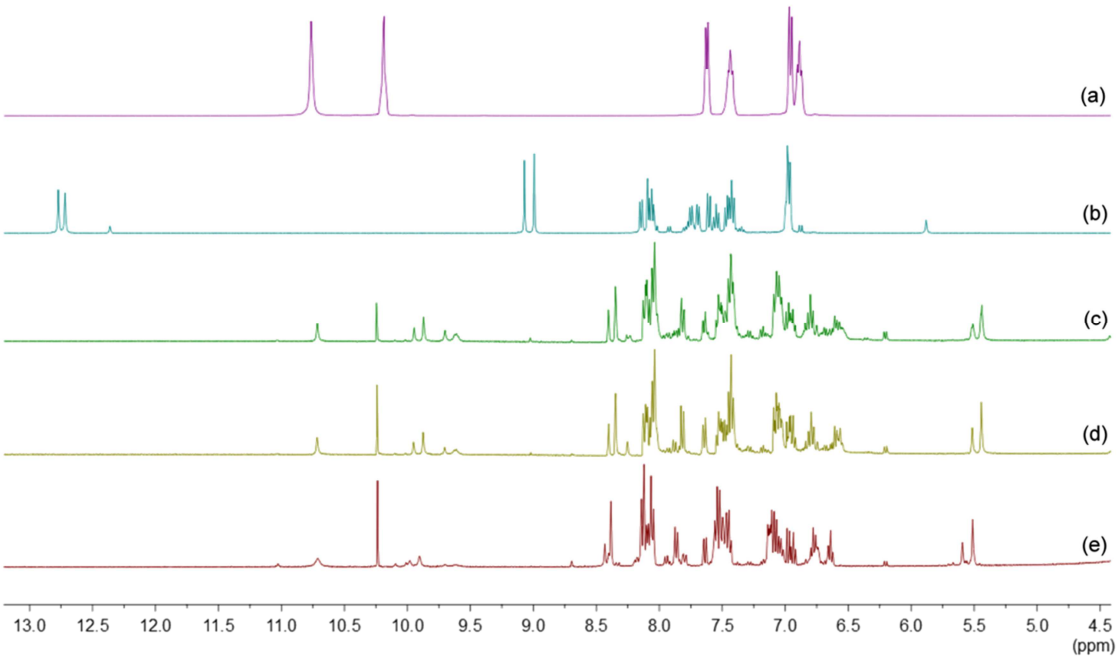

Figure 6. ^{1}H NMR spectra (DMSO-d_6, 400 MHz) of compounds **4** (a) and **6** (b) and **6** with 0.5 (c), 1.0 (d) and 2.0 (e) equivalents of Cu^{2+}.

Upon high amounts of Cu^{2+} the emission shifts drastically to higher energies, below 450 nm. In this case, it is believed that the ligand no longer presents the original structure and the emission is due to the hydrolysed benzothiazole. Further photophysical experiments were performed with the precursor **4** (Table S1, Figures S5 and S6) corroborates with this affirmation, since this compound presents fluorescence emission maxima in the violet to blue regions (430-459 nm) depending on the solvent. Additionally, ESI-MS analysis were also performed to better understand the formed complex between Cu^{2+} and BTS presenting the molar stoichiometry of 1:2 obtained from the Job plot. In this sense, the signal of m/z = 604.9068 related to the $[M+Na]^{+}$ (Figure S8) in which can be observed the isotopic pattern of copper complexes is assigned to the complex illustrated in Scheme 2. Moreover, the product of hydrolysis of BTS, ion peak of m/z = 346.1014 (Figure S9) is also observed. Thus, the presence of an amino group in the ligand structure allows a better interaction of the ligand with the second species of copper. It is worth mentioning that in this proposal it was assumed the reduction of copper(II) during the electrospray ionization step and the formation of copper(I) complex, as already been reported in the literature [51,52].

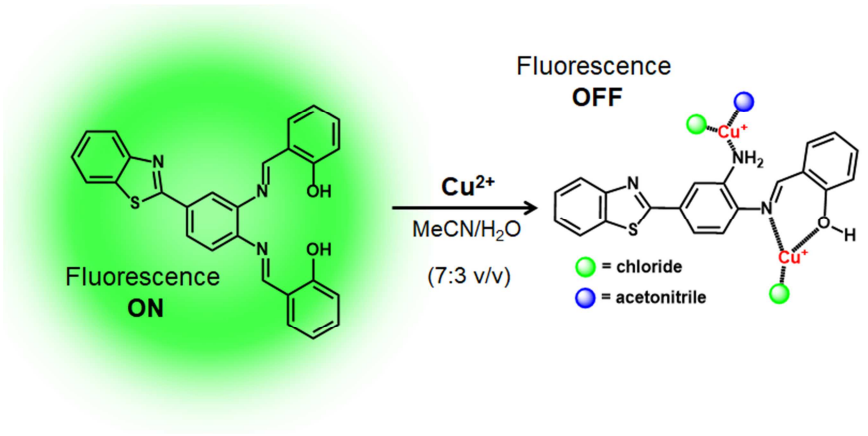

Scheme 2. Proposed chemical mechanism to CHEQ phenomena induced by Cu^{2+} binding, where the blue and green spheres represent acetonitrile molecule and chloride atoms, respectively.

Finally, in order to study a potential application of this process as a CHEQ sensor-based, paper filter strips ~1.0 cm² were immersed in BTS solution, dried in air and then immersed in all metal ions salt solutions. After drying in air again for a few minutes, samples were exposed to UV-lamp illumination (Figure 7). Fluorescence quenching was observed only on the strip immersed in Cu^{2+} solution.

Figure 7. Picture of the emission of paper strips after their immersion in the BTS solution (top) and in each salt solution (bottom) with the exposure to UV-lamp light.

Conclusions

In conclusion, it was described a new application of the ESIPT reactive compound BTS. The synthesised compound presented great sensitivity to copper (II) ions in solution due to a chelation mechanism that inhibits proton transfer on the electronic excited state. This quenching was also evaluated for several metallic ions tested in the mixture $MeCN/H_2O$ (7:3 v/v). In this condition, only Cu^{2+} coordinated successfully and offered pronounced changes of spectral emission, originated from coordination compound with one molecule of BTS partially hydrolysed and two Cu^{2+} ions. This was, further corroborated by ^1H NMR, FTIR and ESI-MS experiments. The

photophysical experiments also offered the binding constant in the order of 10^{10} mol^{-2} L^2 and the limits of detection and quantification of copper (II) as 32 ppb and 108 ppb.

Appendix A. Supporting Information

^{1}H NMR, FTIR and HRMS spectra, Supplementary photophysical data.

Author Information

Corresponding Author

*tatvars@unicamp.br

Authors Contribution

The manuscript was written through contributions of all authors. All authors have given approval to the final version of the manuscript.

Acknowledgements

The authors are thankful for financial support and scholarships from CNPq, CAPES - Financial Code 001, FAPESP 2013/16245-2, FAEPEX and INEO.

References

[1] Pessoa JP, Correia, I. Salan vs. salen metal complexes in catalysis and medicinal applications: Virtues and pitfalls. Coord Chem Rev 2019;388:227-247.

[2] Cozzi PG. Metal–Salen Schiff base complexes in catalysis: practical aspects. Chem Soc Rev 2001;33:410-421.

[3] Shaw S, White JD. Asymmetric catalysis using chiral Salen−metal complexes: Recent advances. Chem Rev 2019;119:9381-9426.

[4] Cozzi PG, Dolci LS, Garelli A, Montalti M, Prodi L, Zaccheroni N. Photophysical properties of Schiff-base metal complexes. New J Chem 2003;27:692-697.

[5] Tuo S, Cattin L, Essaidi H, Peres L, Louarn G, El Jouad Z, Hssein M, Touihri S, Abbe SY, Torchio P, Addou M, Bernède, JC. Stabilisation of the electrical and optical properties of dielectric/Cu/dielectric structures through the use of efficient dielectric and Cu:Ni alloy. J Alloys Compd 2017;729:109-116.

[6] Chen S, Brown L, Levendorf M, Cai W, Ju SY, Edgeworth J, Li X, Magnuson CW, Velamakanni A, Piner RD, Kang J, Park J, Ruoff RS. Oxidation resistance of graphene-coated Cu and Cu/Ni alloy. ACS Nano 2011;5:1321-1327

[7] Bernal M, Casero D, Singh V, Wilson GT, Grande A, Yang H, Dodani SC, Pellegrini M, Huijser P, Connolly EL, Merchant SS, Kramer U. Transcriptome sequencing identifies *SPL7*-regulated copper acquisition genes *FRO4*/*FRO5* and the copper dependence of iron homeostasis in *Arabidopsis.* Plant Cell 2012;24:738-761.

[8] Gaetke LM, Chow CK. Copper toxicity, oxidative stress, and antioxidant nutrients. Toxicology 2003;189:147-163.

[9] Linder MC, In Biochemistry of copper, Springer Science+Business Media, New York, 1991.

[10] Cotruvo JA, Aron AT, Ramos-Torres KM, Chang CJ. Synthetic fluorescent probes for studying copper in biological systems. Chem Soc Rev 2015;44:4400-4414.

[11] Grass G, Rensing C, Solioz M. Metallic copper as an antimicrobial surface. Appl Environ Microbiol 2011;77:1541-1547.

[12] Yruela I. Transition metals in plant photosynthesis. Metallomics 2013;5:1090-1109.

[13] D'Ambrosi N, Rossi L. Copper at synapse: Release, binding and modulation of neurotransmission. Neurochem Int 2015;90:36-45.

[14] Yruela I. Copper in plants: acquisition, transport and interactions. Funct Plant Biol 2009;36:409-430.

[15] Nevitt T, Öhrvik H, Thiele DJ. Charting the travels of copper in eukaryotes from yeast to mammals. Biochim Biophys Acta Mol Cell Res 2012;1823:1580-1593.

[16] Kalita J, Kumar V, Misra UK, Bora HK. Memory and learning dysfunction following copper toxicity: biochemical and immunohistochemical Basis. Mol Neurobiol 2017;55:3800-3811.

[17] Harikrishnan VK, Basheer SM, Joseph N, Sreekanth A. Colorimetric and fluorimetric response of salicylaldehyde dithiosemicarbazone towards fluoride, cyanide and copper ions: Spectroscopic and TD-DFT studies. Spectrochim Acta A Mol Biomol Spectrosc 2017;182:160-167.

[18] Adrees M, Ali S, Rizwan M, Ibrahim M, Abbas F, Farid M, Zia-ur-Rehman M, Irshad MK, Bharwana SA. The effect of excess copper on growth and physiology of important food crops: A review. Environ Sci Pollut Res 2015;22:8148-8162.

[19] Udhayakumari D, Naha S, Velmathi S. Colorimetric and fluorescent chemosensors for Cu^{2+}. A comprehensive review from the years 2013-15. Anal Methods 2017;9:552-578.

[20] Kaushik R, Ghosh A, Singh A, Gupta P, Mittal A, Jose DA. Selective detection of cyanide in water and biological samples by an off-the-shelf compound. ACS Sens 2016;1:1265-1271.

[21] Sakunkaewkasem S, Petdum A, Panchan W, Sirirak J, Charoenpanich A, Sooksimuang T, Wanichacheva N. Dual-analyte fluorescent sensor based on [5]helicene derivative with super large Stokes shift for the selective determinations of Cu^{2+} or Zn^{2+} in buffer solutions and its application in a living cell. ACS Sens 2018;3:1016-1023.

[22] Wu W, Chen A, Tong L, Qing Z, Langone KP, Bernier WE, Jones WE. Facile synthesis of fluorescent conjugated polyelectrolytes using polydentate sulfonate as highly selective and sensitive Copper(II) sensors. ACS Sens 2017;2:1337-1344.

[23] Liu Z, Yang Z, Li T, Wang B, Li Y, Qin D, Wang M, Yan M. An effective Cu(II) quenching fluorescence sensor in aqueous solution and 1D chain coordination polymer framework. Dalton Trans 2011;40:9370-9373.

[24] Mahapatra AK, Mondal S, Manna SK, Maiti K, Maji R, Uddin MR, Mandal S, Sarkar D, Mondal TK, Maiti DK. A new selective chromogenic and turn-on fluorogenic probe for copper(II) in solution and vero cells: recognition of sulphide by [CuL]. Dalton Trans 2015;44:6490-6501.

[25] Qu L, Yin C, Huo F, Zhang Y, Li Y. A commercially available fluorescence chemosensor for copper ion and its application in bioimaging. Sensor Actuat B Chem 2013;183:636-640.

[26] Zhang H, Feng L, Jiang Y, Wong YT, He Y, Zheng G, He J, Tan Y, Sun H, Ho D. A reaction-based near-infrared fluorescent sensor for Cu^{2+} detection in aqueous buffer and its application in living cells and tissues imaging. Biosens Bioelectron 2017;94:24-29.

[27] Zhang B, Liu H, Wu F, Hao GF, Chen Y, Tan C, Tan Y, Jiang Y. A dual-response quinoline-based fluorescent sensor for the detection of copper (II) and iron(III) ions in aqueous medium. Sensor Actuat B Chem 2017;243:765-774.

[28] Zeng L, Miller EW, Pralle A, Isacoff EY, Chang CJ. A selective turn-on fluorescent sensor for imaging copper in living cells. J Am Chem Soc 2006;128:10-11.

[29] Taki M, Iyoshi S, Ojida A, Hamachi I, Yamamoto Y. Development of highly sensitive fluorescent probes for detection of intracellular copper(I) in living systems. J Am Chem Soc 2010;132:5938-5939.

[30] Zhou M, Wang X, Huang K, Huang Y, Hu S, Zeng W. A fast, highly selective and sensitive dansyl-based fluorescent sensor for copper (II) ions and its imaging application in living cells. Tetrahedron Lett 2017;58:991-994.

[31] Shao N, Zhang Y, Cheung SM, Yang RH, Chan WH, Mo T, Li KA, Liu F. Copper ion-selective fluorescent sensor based on the inner filter effect using a spiropyran derivative. Anal Chem 2005;77:7294-7303.

[32] Ferraresso LG, de Arruda EGR, de Moraes TPL, Fazzi RB, Ferreira AMC, Abbehausen C. Copper(II) and zinc(II) dinuclear enzymes model compounds: The nature of the metal ion in the biological function. J Mol Struct 2017;1150:316-328.

[33] Yang X, Zhang W, Yi Z, Xu H, Wei J, Hao L. Highly sensitive and selective fluorescent sensor for copper(II) based on salicylaldehyde Schiff-base derivatives with aggregation induced emission and mechanoluminescence. New J Chem 2017;41:11079-11088.

[34] Ramdass A, Sathish V, Velayudham M, Thanasekaran P, Umapathy S, Rajagopal S. Luminescent sensor for copper(II) ion based on imine functionalized monometallic rhenium(I) complexes. Sensor Actuat B Chem 2017;240:1216-1225.

[35] Situ B, Zhao J, Lv W, Liu J, Li H, Li B, Chai Z, Cao N, Zheng L. Naked-eye detection of copper(II) ions by a “clickable” fluorescent sensor. Sensor Actuat B Chem 2017;240:560-565.

[36] Kar C, Adhikari MD, Datta BK, Ramesh A, Das G. A CHEF-based biocompatible turn on ratiometric sensor for sensitive and selective probing of Cu^{2+}. Sensor Actuat B Chem 2013;188:1132-1140.

[37] Liu C, Wang F, Xiao T, Chi B, Wu Y, Zhu D, Chen X. The ESIPT fluorescent probes for N_2H_4 based on benzothiazol and their applications for gas sensing and bioimaging. Sensor Actuat B Chem 2018;256:55-62.

[38] Geranmayeh S, Mohammadnejad M, Mohammadi S. Sonochemical synthesis and characterization of a new nano Ce(III) coordination supramolecular compound; highly sensitive direct fluorescent sensor for Cu^{2}. Ultrason Sonochem 2018;40:453-459.

[39] Zhou F, Wang H, Liu P, Hu Q, Wang Y, Liu C, Hu J. A highly selective and sensitive turn-on probe for aluminum(III) based on quinoline Schiff's base and its cell imaging. Spectrochim Acta A Mol Biomol Spectrosc 2018;190:104-110.

[40] Feng L, Shi W, Ma J, Chen Y, Kui F, Hui Y, Xie Z. A novel thiosemicarbazone Schiff base derivative with aggregation-induced emission enhancement characteristics and its application in Hg^{2+} detection. Sensor Actuat B Chem 2016;237:563-569.

[41] Li K, Feng Q, Niu G, Zhang W, Li Y, Kang M, Xu K, He J, Hou H, Tang BZ. Benzothiazole-based AIEgen with tunable excited-state intramolecular proton transfer and restricted intramolecular rotation processes for highly sensitive physiological pH sensing. ACS Sens 2018;3:920-928.

[42] Bergonzi R, Fabbrizzi L, Licchelli M, Mangano C. Molecular switches of fluorescence operating through metal centred redox couples. Coord Chem Rev 1998;170:31-46.

[43] Yang W, Chen X, Su H, Fang W, Zhang Y. The fluorescence regulation mechanism of the paramagnetic metal in a biological HNO sensor. Chem Commun 2015;51:9616-9619.

[44] Duarte LGTA, Germino JC, Berbigier JF, Barboza CA, Faleiros MM, Simoni DA, Galante MT, de Holanda MS, Rodembusch FS, Atvars TDZ. White-light generation from all-solution-processed OLEDs using a benzothiazole–Salophen derivative reactive to the ESIPT process. Phys Chem Chem Phys 2019;21:1172-1182.

[45] Armarego WLF, In Purification of Laboratory Chemicals, 5th ed.; Elsevier Academic Press: Cornwall, UK, 2003.

[46] Shrivastava A, Gupta V. Methods for the determination of limit of detection and limit of quantitation of the analytical methods. Chron Young Sci 2011;2:21-25.

[47] Coelho FL, Campo LF. Synthesis of 2-arylbenzothiazoles via direct condensation between *in situ* generated 2-aminothiophenol from disulfide cleavage and carboxylic acids. Tetrahedron Lett 2017;58:2330-2333.

[48] Valeur B. In Molecular Fluorescence Principles and Applications. 1st ed. Wiley-VCH Verlag GmbH, 2000.

[49] Soliman AA, Linert W. Structural features of ONS-donor Salicylidene Schiff base complexes. Monatsh Chem 2007;138:175-189.

[50] Leoni L, Cort AD. The supramolecular attitude of metal–Salophen and metal–Salen complexes. Inorganics 2018;6:42-59.

[51] Gianelli L, Amendola V, Fabbrizzi L, Pallavicini P, Mellerio GG. Investigation of reduction of Cu(II) complexes in positive-ion mode electrospray mass spectrometry. Rapid Commun Mass Spectrom 2001;15:2347-2353.

[52] McIndoe JS, Vikse KL. Assigning the ESI mass spectra of organometallic and coordination compounds. J Mass Spectrom 2019;54:466-479.

Highlights

- Novel fluorescent sensor for Cu^{2+} by Chelation Enhancement Quenching Effect;
- Cu^{2+} detection by quenching of ESIPT process;
- The detection limits for Cu^{2+} were 32 ppb;
- Experimental photophysical properties further compared with ^{1}H NMR and HRMS.

Declaration of interests

☒ The authors declare that they have no known competing financial interests or personal relationships that could have appeared to influence the work reported in this paper.

☐The authors declare the following financial interests/personal relationships which may be considered as potential competing interests: